Janus-faced liposomes enhance antimicrobial innate immune response in *Mycobacterium tuberculosis* infection

Emanuela Greco[a,1], Gianluca Quintiliani[a,1], Marilina B. Santucci[a], Annalucia Serafino[b], Anna Rita Ciccaglione[c], Cinzia Marcantonio[c], Massimiliano Papi[d], Giuseppe Maulucci[d], Giovanni Delogu[e], Angelo Martino[f], Delia Goletti[f], Loredana Sarmati[g], Massimo Andreoni[g], Alfonso Altieri[h], Mario Alma[h], Nadia Caccamo[i], Diana Di Liberto[i], Marco De Spirito[d], Nigel D. Savage[j], Roberto Nisini[c], Francesco Dieli[i], Tom H. Ottenhoff[j], and Maurizio Fraziano[a,2]

Departments of [a]Biology and [g]Clinical Infectious Diseases, University of Rome "Tor Vergata," 00133 Rome, Italy; [b]Institute of Translational Pharmacology, National Research Council, 00133 Rome, Italy; [c]Department of Infectious, Parasitic, and Immunomediated Diseases, Istituto Superiore di Sanità, 00161 Rome, Italy; Institutes of [d]Physics and [e]Microbiology, Catholic University of Sacred Heart, 00168 Rome, Italy; [f]Department of Epidemiology and Preclinical Research, National Institute of Infectious Diseases "Lazzaro Spallanzani," 00149 Rome, Italy; [h]Unit of Tisiology and Bronchopneumology, S. Camillo-Forlanini Hospital, 00151 Rome, Italy; [i]Department of Biopathology and Medical and Forensics Biotechnologies, University of Palermo, 90135 Palermo, Italy; and [j]Department of Infectious Diseases, Leiden University Medical Center, 2333 ZA, Leiden, The Netherlands

Edited by Barry R. Bloom, Harvard School of Public Health, Boston, MA, and approved March 30, 2012 (received for review January 19, 2012)

We have generated unique asymmetric liposomes with phosphatidylserine (PS) distributed at the outer membrane surface to resemble apoptotic bodies and phosphatidic acid (PA) at the inner layer as a strategy to enhance innate antimycobacterial activity in phagocytes while limiting the inflammatory response. Results show that these apoptotic body-like liposomes carrying PA (ABL/PA) (*i*) are more efficiently internalized by human macrophages than by nonprofessional phagocytes, (*ii*) induce cytosolic Ca^{2+} influx, (*iii*) promote Ca^{2+}-dependent maturation of phagolysosomes containing *Mycobacterium tuberculosis* (MTB), (*iv*) induce Ca^{2+}-dependent reactive oxygen species (ROS) production, (*v*) inhibit intracellular mycobacterial growth in differentiated THP-1 cells as well as in type-1 and -2 human macrophages, and (*vi*) down-regulate tumor necrosis factor (TNF)-α, interleukin (IL)-12, IL-1β, IL-18, and IL-23 and up-regulate transforming growth factor (TGF)-β without altering IL-10, IL-27, and IL-6 mRNA expression. Also, ABL/PA promoted intracellular killing of *M. tuberculosis* in bronchoalveolar lavage cells from patients with active pulmonary tuberculosis. Furthermore, the treatment of MTB-infected mice with ABL/PA, in combination or not with isoniazid (INH), dramatically reduced lung and, to a lesser extent, liver and spleen mycobacterial loads, with a concomitant 10-fold reduction of serum TNF-α, IL-1β, and IFN-γ compared with that in untreated mice. Altogether, these results suggest that apoptotic body-like liposomes may be used as a Janus-faced immunotherapeutic platform to deliver polar secondary lipid messengers, such as PA, into phagocytes to improve and recover phagolysosome biogenesis and pathogen killing while limiting the inflammatory response.

Host phospholipids play a critical role in the activation of the antimicrobial innate immune response (1). In particular, phospholipase D (PLD) activation is necessary for intracellular killing of pathogens induced by natural ligands, such as ATP (2, 3), and by microbial ligands, such as CpG oligodeoxynucleotides (4). Interestingly, *Mycobacterium tuberculosis* (MTB), unlike the nonpathogenic *Mycobacterium smegmatis*, inhibits PLD activation during phagocytosis, a process that is associated with intracellular survival of the pathogen (4). PLD catalyzes the hydrolysis of the membrane phospholipid, phosphatidylcholine, to generate the metabolically active phosphatidic acid (PA). PA is an important second messenger involved in multiple physiological functions, including (*i*) the assembly and activation of NADPH oxidase, (*ii*) the regulation of cytoskeleton organization, and (*iii*) the modulation of the vesicular trafficking and membrane fission/fusion events, responsible for phagocytosis and phagolysosome maturation (1, 5). MTB has been also reported to block phagolysosome maturation by inhibiting host sphingosine kinase (6) and phosphatidylinositol 3-kinase activity (7), both involved in different steps of phagolysosome biogenesis. A report by Anes et al. showed that different bioactive lipids, like arachidonic acid (AA), ceramide (Cer), sphingosine (Sph), sphingomyelin (SM), phosphatidylinositol (PI), and sphingosine 1-phosphate (S1P), promoted phagolysosome maturation and intracellular mycobacterial killing in murine macrophages (8). In the same context, we have previously demonstrated that lysophospholipids, such as S1P and lysophosphatidic acid (LPA), (*i*) promote in vitro PLD-dependent phagolysosome maturation and PLD-dependent intracellular killing of MTB in human macrophages (9) and type II alveolar epithelial cell line A549 (10), (*ii*) induce ex vivo intracellular killing of endogenous mycobacteria in bronchoalveolar lavage cells isolated from patients affected by tuberculosis (TB) (11, 12), and (*iii*) reduce in vivo pulmonary mycobacterial burden and histopathology in murine models of TB (9, 13).

Phospholipids may also play a critical role in cell-to-cell signaling. In this context, the exposure of phosphatidylserine (PS) (14, 15), on the outer leaflet of plasma membrane represents one of the most striking and consistent changes of apoptotic cells. Exposure of PS plays a central role in the recognition and phagocytosis of apoptotic bodies by macrophages (16). The functional consequence of a PS-dependent recognition and ingestion of apoptotic cells by macrophages is the release of antiinflammatory cytokines and the inhibition of the production of proinflammatory cytokines (17). These features have highlighted the possibility of using apoptotic cells to manipulate the immune response for therapeutic gain to reduce the immunopathology (18).

The purpose of the present study was to evaluate the possibility of recovering or strengthening antibacterial innate immune responses by providing PA, involved in phagolysosome biogenesis, using liposomes as a vehicle. In this context, the possibility of

Author contributions: A.R.C., M.D.S., N.D.S., R.N., F.D., T.H.O., and M.F. designed research; E.G., G.Q., M.B.S., A.S., C.M., M.P., G.M., A.M., N.C., and D.D.L. performed research; G.D. contributed new reagents/analytic tools; A.R.C., D.G., L.S., M. Andreoni, A.A., M. Alma, M.D.S., N.D.S., R.N., F.D., T.H.O., and M.F. analyzed data; and N.D.S., R.N., F.D., T.H.O., and M.F. wrote the paper.

Conflict of interest statement: E.G., G.Q., M.D.S., and M.F. are named on a patent application for work described in this paper.

This article is a PNAS Direct Submission.

[1]E.G. and G.Q. contributed equally to this work.

[2]To whom correspondence should be addressed. E-mail: Fraziano@bio.uniroma2.it.

See Author Summary on page 7963 (volume 109, number 21).

This article contains supporting information online at www.pnas.org/lookup/suppl/doi:10.1073/pnas.1200484109/-/DCSupplemental.

engineering liposomes characterized by the expression of different phospholipids at the outer and inner membrane surface has been described (19) and offers a technological platform to asymmetrically distribute bioactive phospholipids involved in different cell functions. On these grounds, we have generated unique asymmetric apoptotic body-like liposomes (ABL), with PS distributed at the outer membrane surface to resemble apoptotic bodies, thus targeting macrophages while limiting inflammation, and with PA at the inner membrane surface to simultaneously enhance phagolysosome biogenesis-related processes. These double-faced liposomes were tested for their potential enhancing effect on innate immunity functions and bacterial killing.

Results

Biophysical Characterization of Liposomes. To check the asymmetric distribution of phospholipids in liposome preparations, we first stained liposomes with Cy5-Annexin V and monitored fluorescence emission distribution on the outer surface of liposome membrane by flow cytometry analysis. The results show the presence of Annexin V binding sites on the liposome surface in ABL/PA, visualized by increased fluorescence emission after Cy5-Annexin V staining (Fig. S1*A*). To demonstrate the presence of PA within liposomes, ABL carrying 1-myristoyl-2-{12-[(7-nitro-2–1,3-benzoxadiazol-4-yl)amino]lauroyl}-*sn*-glycero-3-phosphate (NBD-PA) (a fluorescent PA analog) were analyzed by confocal microscopy. The results, shown in Fig. S1*B*, reveal the presence of PA inside the liposome membrane. The level of asymmetry of phospholipids is further confirmed when NBD-PA is incorporated either inside the liposome membrane (PS/NBD-PA) or at the outer liposome surface (NBD-PA/PS) (Fig. S1*C*). In the first case, on addition of the quencher, the signal decreases ∼9% but it drops ∼65% when NBD-PA is incorporated at the outer leaflet. These results demonstrate that ∼90% of NBD-PA is confined at the inner liposome surface when it is produced as PS/NBD-PA and that ∼65% of NBD-PA is distributed at the outer surface when it is produced as NBD-PA/PS, according to a natural tendency exerted by PA to distribute within the liposome surface (20).

The liposome's size has been tested by using dynamic light scattering. The mean hydrodynamic radius is reported for all of the preparations investigated [ABL/phosphatidylcholine (PC), PC/PC, PC/PA, and ABL/PA] in Fig. S1*D*. All of the samples show a hydrodynamic radius of ∼1 μm with the exception of the ABL/PC sample whose radius is 2.5 μm, which could reflect the interaction between PS and PC that modifies the thermodynamic equilibrium by shifting the mean radius toward larger values (21).

Internalization of ABL/PA and Inhibition of Proinflammatory Responses. The ability of ABL carrying NBD-PA (PS/NBD-PA) to be phagocytosed by Phorbol 12-Myristate 13-Acetate (PMA) differentiated THP-1 (dTHP-1) cells was analyzed by confocal microscopy and compared with control liposomes expressing PC at the outer leaflet of the liposome surface (PC/NBD-PA) (Fig. 1). As expected the expression of PS at the outer liposome surface (PS/NBD-PA) induces liposome internalization within macrophages (Fig. 1*A*), which is significantly enhanced, in comparison with PC/NBD-PA liposome preparations (Fig. 1*B*). In agreement, the frequency of ABL/NBD-PA liposomes phagocytosed by macrophages was higher than that observed with PC/NBD-PA also if FBS was replaced by human AB+ serum (Fig. S1*E*). When the uptake of ABL by dTHP-1 cells was compared with that by alveolar epithelial A549 cells, primary monocyte-derived macrophages (MDM), and type-1 (M1) and type-2 (M2) macrophages, results showed that the percentage of ABL/PA phagocytosed was significantly higher in macrophages than in A549 cells, with the highest phagocytic capability being exerted by primary macrophages (Fig. 1*C*). Finally, the possible toxic effect by the different liposome preparations was assessed in terms of cell viability analyzed by trypan blue exclusion (Fig. S2*A*) and 3-(4,5-Dimethylthiazol-2-yl)-2,5-diphenyltetrazolium bromide (MTT) assay (Fig. S2*B*). Results show that liposomes are not toxic because no difference in cell viability is obtained after exposure of the cells to the different liposome preparations.

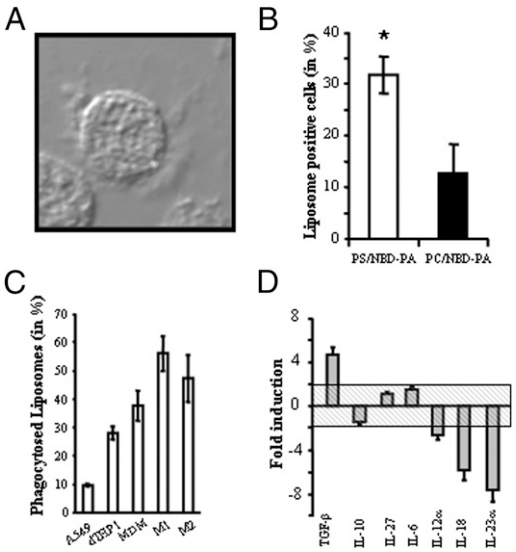

Fig. 1. Internalization of ABL/PA and inhibition of proinflammatory response in human macrophages. (*A*) dTHP-1 cells were stimulated with the same number of ABL carrying NBD-PA for 90 min and phagocytosis was analyzed by confocal fluorescence microscopy. (*B*) Summary of the mean percentage ± SD of dTHP-1 cells with at least one liposome internalized over total cells by counting ≥100 dTHP-1 cells per sample. Three different experiments were assessed. *P = 0.003 by Student's t test. (*C*) Comparative analysis of internalization of ABL carrying NBD-PA in A549 cells, dTHP-1 cells, monocyte-derived macrophages (MDM), type 1 macrophages (M1), and type 2 macrophages (M2). Results are expressed as mean ± SD of three independent determinations (for A549 and dTHP-1 cells) and three different donors (for MDM, M1, and M2 cells). (*D*) dTHP-1 cells were stimulated with the same number of ABL/PA for 18 h and then analyzed by real-time PCR for detection of cytokine mRNA levels. Values of fold induction were the means ± SD of three independent cellular experiments, each performed by pooling of mRNA from at least three biological replicates derived by cells seeded in different plates.

We next monitored mRNA expression of representative proinflammatory and antiinflammatory cytokines by real-time PCR in dTHP-1 cells, stimulated or not with ABL/PA. The results expressed in Fig. 1*D* show that after 24 h of liposome treatment, most proinflammatory cytokine mRNAs [interleukin (IL)-12-α, IL-18, and IL-23-α] were down-regulated (−2.60-, −5.80-, and −7.60-fold, respectively) in comparison with untreated cells whereas IL-10, IL-27, and IL-6 mRNAs were not altered after treatment (fold inductions between ±2). By contrast, transforming growth factor (TGF)-β mRNA was strongly up-regulated (+4.66-fold induction) after exposure of macrophages with ABL/PA.

ABL/PA Limit Inflammatory Responses and Enhance Intracellular Mycobacterial Killing in the Course of in Vitro *M. tuberculosis* Infection. To evaluate proinflammatory vs. antiinflammatory properties of ABL/PA in the course of in vitro MTB infection, we measured the production of tumor necrosis factor (TNF)-α, IL-1β, and TGF-β in the supernatant of dTHP-1 cells, infected or not with MTB and in the presence or absence of liposomes, 72 h after infection (Fig. 2*A*). As expected, both IL-1β and TNF-α were strongly up-regulated after MTB infection and ABL/PA slightly, although significantly, reduced their release. By contrast, TGF-β production was significantly up-regulated in MTB-infected liposome-treated macrophages in comparison with MTB-

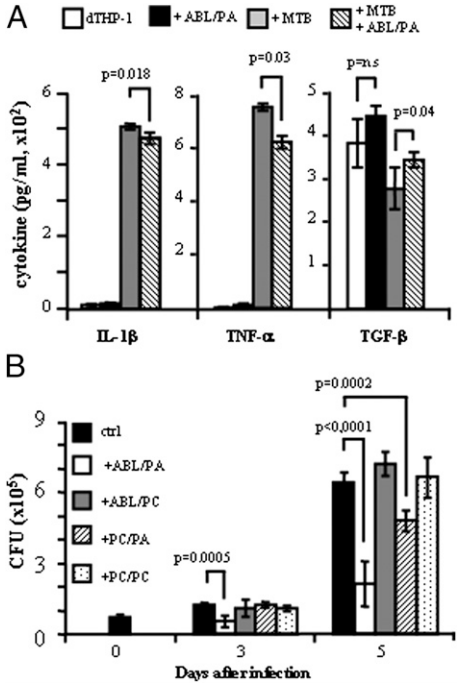

Fig. 2. ABL/PA modulate proinflammatory response and induce intracellular mycobacterial killing in human macrophages. (*A*) Levels of IL-1β, TNF-α, and TGF-β were analyzed in the supernatant of dTHP-1 cells infected or not with MTB at the MOI of 1 and stimulated or not with ABL/PA liposomes at 72 h after infection and stimulation. (*B*) dTHP-1 cells were infected with MTB at the MOI of 1 and then stimulated, for 3 and 5 d, with the same amount of the following liposomes: (*i*) phosphatidylserine outside/phosphatidic acid inside (ABL/PA), (*ii*) phosphatidylserine outside/phosphatidylcholine inside (ABL/PC), (*iii*) phosphatidylcholine outside/phosphatidic acid inside (PC/PA), and (*iv*) phosphatidylcholine outside/phosphatidylcholine inside (PC/PC). Results are expressed as means ± SD of triplicate values and are representative of three separate experiments. Differences were evaluated by Student's *t* test.

infected controls; a slight, but not significant, increase in TGF-β was observed in liposome-treated macrophages in comparison with untreated cells.

We next tested the capability of ABL/PA to increase the mycobacterial killing activity of dTHP-1 cells. Results (Fig. 2*B*) show a significant reduction of intracellular mycobacterial viability after treatment with ABL/PA. A lesser, although still significant, reduction of intracellular mycobacterial growth was also observed after stimulation with liposomes expressing PC outside/PA inside (PC/PA), in agreement with the different ability of phagocytes to internalize these two types of liposomes (Fig. 1*B*). Finally, the antimycobacterial effect was specifically induced by PA as no effect was observed after stimulation with ABL/PC. Altogether, these results highlight PA as the component modulating the antimycobacterial function of macrophages.

ABL/PA Promote Ca^{2+}-Dependent Phagolysosome Maturation. Intracellular calcium increase is required for many different signal transduction pathways, including activation of antimycobacterial responses (22, 23). We therefore analyzed cytosolic Ca^{2+} influx in dTHP-1 cells following stimulation with ABL/PA. Results show an immediate increase of cytosolic Ca^{2+} after ABL/PA treatment (Fig. 3*A*), peaking at ~3 min after stimulation (889.5 nM). Cytosolic Ca^{2+} after ABL/PA stimulation was almost completely inhibited by the presence of ethylene glycol tetraacetic acid (EGTA) and 1,2-bis(2-aminophenoxy)ethane-*N*,*N*,*N*′,*N*′-tetraacetic acid acetoxymethyl ester (BAPTA-AM), used as extracellular and intracellular Ca^{2+} chelators, respectively (Fig. S3 *A* and *B*). A progressive reduction in the peak of cytosolic Ca^{2+} was observed following stimulation with ABL/PC (527.6 nM), PC/PA (122.2 nM), and PC/PC (96.3 nM) control liposomes (Fig. S3 *C*–*E*). Moreover, the results indicate that the presence of PS on the outer liposomal surface promotes Ca^{2+} mobilization at 20 min after stimulation whereas the presence of PA within ABL maintained Ca^{2+} mobilization up to 40 min (Fig. S3*F*).

As MTB is known to reside in immature endosomal compartments sequestered from late endosomes/lysosomes (24–26), the maturation of MTB-containing vacuoles and its dependence on Ca^{2+} mobilization were investigated in cells stimulated by ABL/PA, in the presence or absence of EGTA, or by PC/PC control liposomes by laser scanning confocal microscopy, using (*i*) Lysosomal-Associated Membrane Protein (LAMP)-1 and LAMP-3 as markers of lysosomes/late endosomes, (*ii*) the acidophilic dye Lysotracker Red, (*iii*) microtubule-associated protein light chain 3 (LC-3) as an autophagy marker, and (*iv*) DQ-BSA to monitor phagolysosomal protease activity. As expected, green fluorescent phagocytosed mycobacteria resided in LAMP-1 negative compartments (Fig. 3*B*), consistent with an immature maturation state of the phagosomes. In contrast, the stimulation with ABL/PA, but not with PC/PC control liposomes, induced the expression of LAMP-1 in phagosomes containing MTB, which now appeared yellow, whereas the addition of EGTA almost completely reversed this process. In Fig. 3*C*, a summary of all percentages of MTB colocalizing in Lysotracker Red, LAMP-1, LAMP-3, LC-3, and DQ-BSA–positive vacuoles over the total intracellular mycobacteria is given (for representative images see Fig. S4 *A*–*D*). The results show the significant increase in phagolysosome maturation following ABL/PA stimulation and the inhibitory effect exerted by the addition of chloroquine [for Lysotracker Red (LTR) staining] or EGTA (for all markers used), indicating that ABL/PA-induced phagolysosome maturation was Ca^{2+} dependent. Moreover, the analysis of LC-3, a specific autophagic membrane marker, suggests that this process overlaps, at least in part, with the autophagolysosome pathway (Fig. S4*C*).

ABL/PA Promote Intracellular Mycobacterial Killing by a Reactive Oxygen Species (ROS)-Dependent and Phagolysosome-Mediated Mechanism. Phagocytes generate ROS by using superoxide-generating NADPH oxidase (NOX) family proteins, which play pivotal roles in host defense against bacterial and fungal pathogens (27). Following stimulation with ABL/PA, a significant increase in ROS production was observed starting from 20 min after stimulation, which remained significantly higher in comparison with that in control liposomes up to 40 min after stimulation (Fig. S5*A*). This increase was almost completely inhibited by the addition of polyethylene glycol-Catalase (PEG-Cat) (Fig. S5*B*). Moreover, because Ca^{2+} mobilization is required for phagolysosome maturation and polymerization of NADPH oxidase occurs on maturing phagosomes (28), we tested the Ca^{2+} dependence of ROS production. A significant abrogation of ROS production was observed in the presence of the extracellular and intracellular Ca^{2+} chelator EGTA and BAPTA-AM, respectively (Fig. S6*A*).

To assess the role of ABL/PA-induced phagolysosome maturation and ROS production in intracellular mycobacterial killing, dTHP-1 cells were infected with MTB, stimulated with liposomes, and then exposed to the lysosomotropic agents chloroquine and NH_4Cl, which both increase intralysosomal pH and are considered to be general lysosomal inhibitors. Results show that the antimycobacterial activity increased by ABL/PA was mediated by phagolysosome maturation and acidification because the addition of chloroquine or NH_4Cl upon ABL/PA treatment significantly reduced intracellular mycobacterial killing, particularly after 5 d of MTB infection (Fig. S6*B*). Moreover, to assess the role of ROS in the ABL/PA-induced intracellular mycobacterial killing, MTB-infected cells were also exposed to

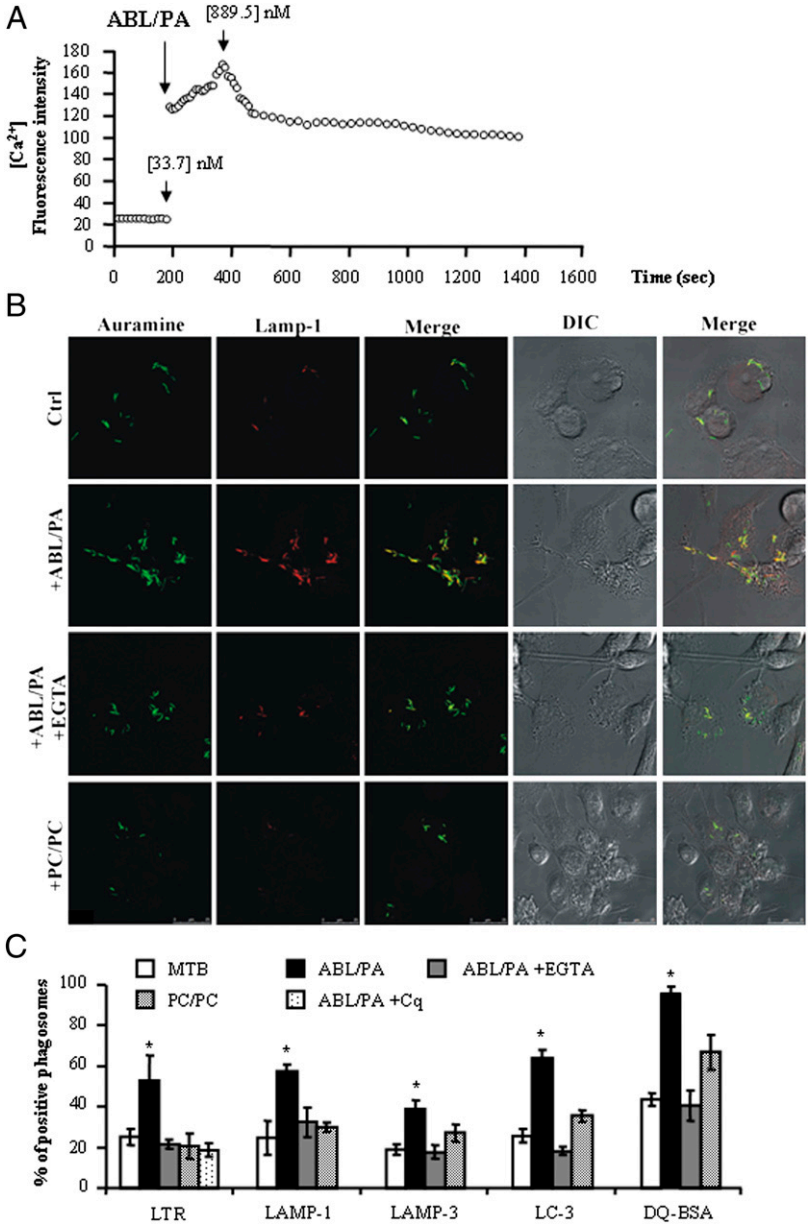

Fig. 3. ABL/PA promote Ca^{2+}-mediated phagolysosome maturation in human macrophages. (*A*) dTHP-1 cells were incubated with 3 μM Fluo-3/AM at 37 °C for 1 h in the dark and were stimulated with ABL/PA or PC/PC control liposomes. After stimulation, fluorescence emission was continuously monitored for 20 min to determine relative alterations in intensity. (*B*) Confocal microscopy representative images (from three separate experiments) showing the increase of Auramine-stained MTB (green) residing in LAMP-1–positive vacuoles (red) after stimulation with ABL/PA. To distinguish signals deriving from internalized MTB and to avoid mycobacteria adhering on the cell surface, Auramine and LAMP-1 signals were obtained from a 3D reconstruction of images taken throughout 1 μm of thickness inside cells. Cell morphology was visualized by differential interference contrast (DIC) and the merged images of the three signals (Auramine/LAMP-1/DIC) were also shown. (*C*) Summary of the mean percentage ± SD of MTB colocalizing in acidic (Lysotracker Red-positive), LAMP-1–, LAMP-3–, LC-3–, or DQ-BSA–positive vacuoles after stimulation with ABL/PA or PC/PC control liposomes and the reverse effect exerted by EGTA or by chloroquine, determined by counting ≥40 phagosomes per sample. Three different experiments were assessed. $*P \leq 0.001$ in comparison with MTB-infected cells.

PEG-Cat, which converts hydrogen peroxide to water and oxygen and thus reduces ROS activity. The results indicate that PEG-Cat almost completely abolishes ABL/PA-induced intracellular MTB killing.

ABL/PA Induce Intracellular (Myco)Bacterial Killing in Primary Type-1 and Type-2 Macrophages and in Bronchoalveolar Lavage Cells. M1 and M2 macrophages have been previously described as proinflammatory and antiinflammatory macrophages (29, 30), respectively, playing different roles during chronic inflammatory pathologies, such as TB (31). Here, we show that stimulation with ABL/PA determines a significant increase in the killing of intracellular MTB by both types of macrophages (Fig. 4*A*) in the absence of any macrophage toxicity (Fig. S7 *A* and *B*). Thus, the effect of ABL/PA is evident not only in human cell lines, but also in primary human macrophages and different subsets thereof.

On the basis of this finding, we wanted to extend our observations to in vivo-infected human macrophages. To reproduce the effect of ABL/PA on cells from the lungs of patients with TB, cells isolated from bronchoalveolar lavage (BAL) of three patients with active sputum-positive pulmonary TB (patients 1, 2, and 3) were stimulated with ABL/PA and cultured for 3 d, and,

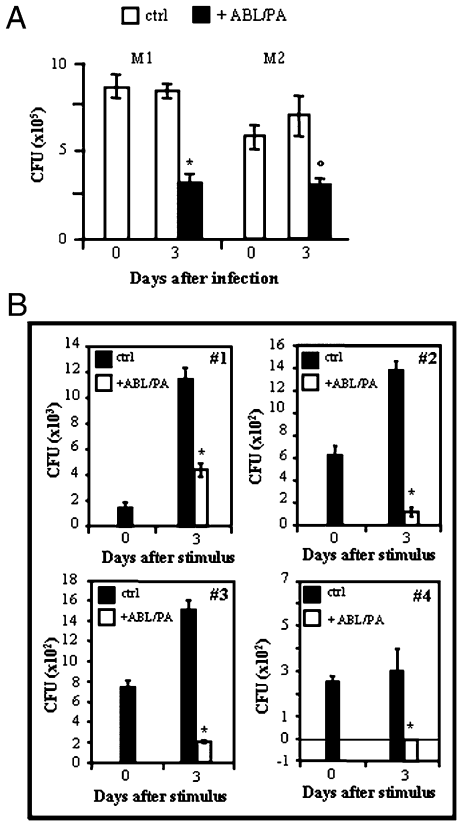

Fig. 4. ABL carrying PA inhibit intracellular (myco)bacterial growth in primary type 1 (M1) and type 2 (M2) macrophages and in bronchoalveolar lavage (BAL) cells. (*A*) M1 and M2 were infected with MTB at the MOI of 1 and then stimulated, for 3 d, with same amount of ABL carrying PA. Data are expressed as means ± SD of triplicate values and are representative of two separate experiments. $*P = 0.00071$, $°P = 0.001$ in comparison with MTB-infected macrophages. (*B*) BAL cells from three patients infected by active pulmonary tuberculosis (patients 1, 2, and 3) and one patient infected by *Klebsiella pneumoniae* (patient 4) were stimulated in vitro with same amount of ABL/PA. A colony-forming unit assay was performed before the addition of ABL/PA and at 72 h after stimulation. Data are expressed as means ± SD of the cfu performed in triplicate. $*P < 0.0001$ in comparison with untreated cells, by Student's *t* test.

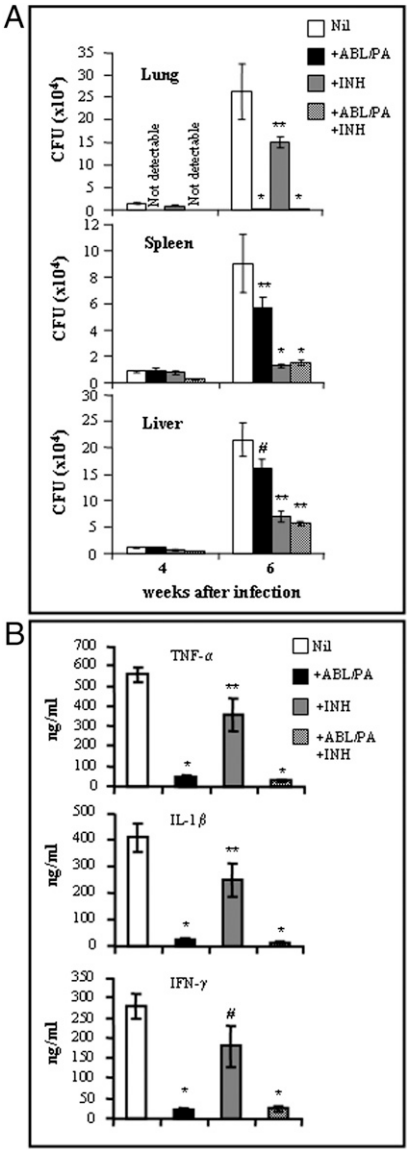

Fig. 5. Therapeutic role of ABL/PA treatment in an experimental model of murine tuberculosis. (*A*) ABL/PA were administrated intranasally three times per week, starting from day 14 after intranasal H37Rv infection, for 4 wk in the presence or absence of isoniazid (INH) provided in the drinking water for the same period. Mycobacterial load of the lung, spleen, and liver is shown as the mean of cfu ± SD obtained from six mice per group at 4 and 6 wk after infection. $*P < 0.001$, $**P < 0.05$, $^{\#}P$ = not significant (NS) in comparison with MTB-infected control mice. (*B*) Serum levels of TNF-α, IL-1β, and IFN-γ were quantified at 6 wk after infection and expressed as means ± SD of values from six mice per group. $*P < 0.001$, $**P < 0.05$, $^{\#}P$ = NS in comparison with MTB-infected control mice.

finally, the growth of intracellular bacteria was monitored by colony-forming unit (cfu) count. In this setting, MTB infection of macrophages and its effects on macrophage differentiation have already occurred in vivo such that this assay represents a model to measure the possible in vivo efficacy of ABL/PA. Fig. 4*B* shows that the treatment of BAL cells from patients 1, 2, and 3 with ABL/PA induced a strong reduction of intracellular MTB. Interestingly, when ABL/PA were tested on BAL from a patient with *Klebsiella* pneumonitis (patient 4), an almost complete eradication of intracellular *Klebsiella pneumoniae* was observed, suggesting that ABL/PA treatment is not MTB specific, but rather increases the general killing activity of macrophages.

Therapeutic Application of ABL/PA in *M. tuberculosis*-Infected Mice Reduces Mycobacterial Load and Inflammatory Response. To test the possible therapeutic effect of ABL/PA in vivo, MTB-infected mice were treated by intranasal administration of ABL/PA, oral administration of isoniazid (INH), or a combination of both, three times per week for 4 consecutive weeks. At the end of the treatment, mycobacterial load in the lung, spleen, and liver was measured as well as serum levels of TNF-α, IL-1β, IFN-γ, lactate dehydrogenase (LDH), alanine transaminase (ALT), aspartate transaminase (AST), and blood urea nitrogen (BUN). Fig. 5*A* reports that treatment with ABL/PA alone or in combination with INH caused at 6 wk after infection (i.e., after 4 wk of treatment) a 100-fold reduction of pulmonary mycobacterial load (1,100 ± 120 cfu and 2,100 ± 500 cfu, respectively), whereas treatment with INH alone caused only a 2-fold reduction of MTB cfu. Interestingly, opposite results were obtained in the spleen and in the liver where ~10-fold reduction was observed following treatment with INH or INH plus ABL/PA and a slight reduction, which was significant only in the spleen, was shown following treatment with ABL/PA only. To test the specificity of the response, we compared the in vivo effect of ABL/PA with

control liposomes (ABL/PC, PC/PA, and PC/PC) in combination with INH, because the combined therapy (ABL/PA plus INH) provided the best results in terms of reduction of mycobacterial burden. Addition of control liposomes to INH therapy did not augment the effect of INH both in the lung and in the spleen. On the other hand, when ABL/PA was used in combination with INH, a 100-fold reduction of mycobacterial burden was observed in the lung (3,800 ± 510 cfu), but, as expected, not in the spleen (Fig. S8*A*).

The therapeutic effect exerted by the treatment with ABL/PA or with ABL/PA plus INH was associated with ~10-fold reduction of TNF-α, IL-1β, and IFN-γ in the serum (Fig. 5*B*) and with a concomitant reduction of LDH, a nonspecific marker of tissue toxicity, and of ALT and AST as parameters of liver toxicity, in comparison with levels in infected untreated mice (Fig. S8*B*). Blood urea nitrogen (as a measure of kidney toxicity) was found unchanged irrespective of the different treatments (Fig. S8*B*).

Discussion

Liposomes are vesicles of varying size consisting of a spherical lipid bilayer, which are useful as carriers to deliver pharmacologically active agents or antigens (32), as they can protect their cargo from the environment until controlled release occurs at the target sites. Moreover, the possibility to asymmetrically distribute bioactive lipids through the liposome membrane provides additional value to liposome-based therapeutic strategies because the cargo of bioactive lipids, used as unique immunomodulators (33), can be preferentially delivered to specific target cells. Here we report a unique study exploring the possibility of using liposomes as carriers of the lipid second messenger PA, known to activate intracellular antimycobacterial signaling (2–5, 9), to promote the antimicrobial response of phagocytes. The preferential targeting of phagocytes is obtained by the expression of PS at the outer leaflet of the liposomal membrane, which makes the liposomes behave as apoptotic bodies.

Macrophages are the primary cells initiating granuloma formation and the major cell type in most granulomas (34, 35). Moreover, they both harbor the majority of MTB bacilli and possess effector functions to kill these bacilli. There are a variety of macrophage phenotypes in granulomas with various functions, including antimycobacterial effector mechanisms, pro- and antiinflammatory cytokine production, and secretion of chemokines and proteins associated with tissue remodeling (29, 30). Thus, these cells contribute to most aspects of inflammation and control of infection within the granuloma. The results reported here show that the presence of PS at the outer leaflet of the liposomal membrane makes the liposomes phagocytosed more efficiently by human macrophages than by alveolar epithelial cells. Our data also show that phagocytosis of ABL/PA is associated with enhanced TGF-β and reduced proinflammatory cytokine expression, such as IL-12, TNF-α, IL-1β, IL-18, and IL-23. In this context, it has been previously shown that phagocytosis of apoptotic bodies is associated with antiinflammatory responses and resolution of inflammation (18, 36). The antiinflammatory effects of apoptotic bodies have also been demonstrated in vivo. Deliberate instillation of apoptotic cells into sites of local inflammation in the lungs and peritoneal cavity increased production of TGF-β and enhanced resolution of injury (37). Moreover, a decrease in alveolar macrophage apoptosis is associated with increased pulmonary inflammation in a murine model of pneumococcal pneumonia (38), and defective clearance of apoptotic cells in CD44 knockout mice leads to unremitting inflammation following noninfectious lung injury (39). On these grounds, our results support the hypothesis that ABL may have the potential to limit inflammation also in an in vivo setting.

The dynamic interactions between MTB and human macrophages are central in all phases of TB, from initial infection to active disease. A crucial feature in TB is the ability of the tubercle bacilli to escape the microbicidal activities of macrophages and to persist as intracellular parasites. In this context, MTB was shown to have evolved a number of mechanisms that contribute to its intracellular survival. These include inhibition of (*i*) PLD-dependent PA generation (4), (*ii*) Ca^{2+} signaling (23), and (*iii*) phagolysosome maturation (40). In particular, PA is involved in the induction of several macrophage antimicrobial activities, such as Ca^{2+} mobilization and actin polymerization, ROS production, and intracellular trafficking of endocytosed immune complexes to lysosomes (41). Moreover, PA mediates phagolysosome maturation in the course of intracellular mycobacterial killing induced by natural and microbial ligands, such as ATP (2), Sphingosine 1-phosphate (9), LPA (12), and CpG oligodeoxinucleotide (22). In this study, we have exploited the possibility of circumventing the reduced PLD activity caused by MTB by providing PA directly to infected macrophages, via asymmetric liposomes. Indeed, we find that PA delivered in the context of ABL promotes Ca^{2+} mobilization, Ca^{2+}-dependent phagolysosome maturation, and intracellular mycobacterial killing, the extent of which is directly related to the liposome internalization capability. The efficient killing of mycobacteria by host macrophages depends on a number of mechanisms, including production of ROS by NOX2, which is assembled from component subunits at the plasma or phagosomal membrane of phagocytes (42). Interestingly, ROS generation was shown to be essential for ABL/PA-induced antimycobacterial activity, resembling the effects of 1,25-dihydroxyvitamin D(3) (43, 44). Finally, autophagy has recently been reported as a possible mechanism concurring with intracellular MTB killing (40). Autophagy was shown to be dependent on (*i*) Ca^{2+} mobilization, via a phosphatidylinositol 3-phosphate–mediated process (40), (*ii*) ROS generation (45), and (*iii*) phospholipase D activity (46). We show here that the phagolysosome maturation process induced by ABL/PA is also associated with the Ca^{2+}-dependent acquisition of the specific autophagic marker LC-3 in the vacuoles containing MTB. Altogether, our findings suggest that Ca^{2+} mobilization, ROS generation, and (auto)phagolysosome maturation represent effector processes induced by ABL/PA that concur with the intracellular killing of MTB.

Macrophages can differentiate into subsets called M1 and M2, respectively, that exhibit distinct biological features in terms of antimicrobial defense, cytokine production, and antigen presentation (47). In particular, M1 macrophages are characterized as having higher expression of class II MHC, CD80, and CD86 and promoting Th1 differentiation and IFN-γ production by T cells via the production of IL-12. Conversely, M2 macrophages, characterized by the up-regulation of scavenger receptors and mannose receptor and by the capability to facilitate tissue repair, produce IL-10 and TGF-β as the prevalent antiinflammatory cytokines and down-regulate Th1 responses (47). In the context of TB, M1-dependent production of proinflammatory mediators and the consequent recruitment and stimulation of T cells can lead to tissue damage and exacerbation of disease (34). As both M1 and M2 cells can be efficiently infected by mycobacteria, it is noteworthy that stimulation with ABL/PA induced intracellular mycobacterial killing in both types of macrophages whose balance in granulomas may be necessary to control infection and tissue damage.

Experiments in the mouse model of TB confirmed the efficacy of the asymmetric liposomes also in vivo. In fact, the combined treatment of MTB-infected mice with ABL/PA (via the intranasal route) plus INH (orally administrated) resulted in a 100-fold reduction of mycobacterial colonies in the lung and a 10-fold reduction in the spleen and liver. The differences in the effects observed in the analyzed organs are likely to represent the different pharmacokinetics of the two compounds. In this context, intranasally administrated ABL/PA may easily reach the lung but may be limited in reaching spleen and liver macrophages. On the

other hand, orally administered INH may reach all organs analyzed with the same efficiency. Antimycobacterial activity enhanced by ABL/PA is also associated with a strong reduction of both serological proinflammatory cytokines and hematological parameters of tissue cytotoxicity, so confirming, in an in vivo experimental model of murine tuberculosis, the double action of ABL/PA.

Of additional importance and high translational relevance, we show that ABL/PA stimulation of BAL cells from TB patients as well as from a patient with *K. pneumoniae* infection induced a significant reduction in bacterial growth of the respective endogenous intracellular pathogen. BAL cells are a mixed cell population and comprise predominantly alveolar macrophages, T lymphocytes, and neutrophils. In this context, the result reported herein on BAL cells is relevant because it indicates that ABL/PA are active in a microenvironment that mirrors that of the infected lung. ABL/PA caused the activation of Ca^{2+}-dependent ROS generation and phagolysosome maturation and these functions were both associated with the reduction/eradication of intracellular MTB and *K. pneumoniae* in BAL cells. As expected from an innate immunity-enhancing compound, the antimicrobial effect induced by ABL/PA does not seem to discriminate between intracellular pathogens and thus may represent a unique strategy to control different microbial pathogens. In fact, induction of ROS-mediated intracellular killing of *K. pneumoniae* has been described following stimulation of alveolar macrophages with leukotrienes (48).

In conclusion, ABL/PA may be considered as Janus-faced liposomes, with an external surface exposing PS, resembling apoptotic bodies and inducing efficient phagocytosis accompanied by the induction of antiinflammatory responses, and with an inner surface containing PA to enhance the antibacterial functions of innate cells. In many long-lasting infections such as TB, the activation of an inefficacious immune response may lead to a chronic inflammation and consequent tissue damage. The possibility of enhancing innate immunity to treat microbial infection by a noninflammatory pathway has been suggested in the past (49). The existing antibiotic regimens against tuberculosis last 6 mo, often resulting in patient noncompliance, treatment failure, infection relapse, and the emergence of drug resistance (26). In this context, the use of ABL/PA may represent an exploitable immunotherapeutic strategy to simultaneously reduce immunopathology and strengthen the innate response against multidrug- or extensively drug-resistant (myco)bacteria.

Materials and Methods

Liposome Preparations. Asymmetric liposomes were produced according to the Pautot et al. method to allow an asymmetric distribution of the outer and inner phospholipids (19). In particular, to prepare the inner monolayer lipid suspension, 2.5 mg of phospholipid and 50 mL of anhydrous dodecane (Sigma) were placed in a 100-mL glass bottle to reach a lipid concentration of 0.05 mg/mL. The suspension was then sonicated in a bath for 30 min and left overnight at room temperature. The following day, 250 μL of an aqueous solution consisting of 100 mM NaCl and 5 mM Tris Buffer, pH 7,4 was added and the solution was stirred with a magnetic stir bar for a further 3 h. To prepare the outer monolayer lipid suspension, 2.5 mg of phospholipid was added to 50 mL of a 99:1 dodecane:silicone solution to get a lipid concentration of 0.05 mg/mL. Thereafter, 2 mL of outer monolayer lipid suspension was added over 3 mL of either PBS or RPMI 1640 in a 50-mL plastic tube (Corning). Finally, 100 μL of the inner monolayer lipid suspension wasadded over the 2-mL lipid phase and the sample was centrifuged at $710 \times g$ for 10 min. After the centrifugation, liposomes were collected in the aqueous phase, using a 5-mL syringe with a 16-gauge stainless steel needle. The following lipids (all from Avanti Polar Lipids) were used for the preparation of the inner and outer monolayers: L-α-phosphatidylserine (PS), L-α-phosphatidylcholine (PC), L-α-phosphatidic acid (PA), and NBD-PA. Liposomes were then quantified by flow cytometry (FACSCalibur; Becton Dickinson), allowing quantification of monodispersed vesicles >0.2 μm in diameter, whereas their mean radius was analyzed by dynamic light scattering analysis (*SI Materials and Methods*).

Bacteria. Pathogenic MTB H37Rv was grown in Middle Brook 7H9 broth supplemented with albumin, dextrose, and catalase. Mycobacteria were then harvested, suspended in sterile PBS, pH 7.2, aliquoted, and stored at −80 °C until use. Before infection, aliquots were grown on 7H10 plates to titer the bacteria after thawing.

Cell Cultures. The human promonocytic THP-1 leukemia cell line, induced to differentiate by stimulation with PMA, was used as a model of human macrophages. Cells were grown in complete medium (RPMI 1640 supplemented with 10% (vol/vol) FBS, 2 mM L-glutamine, and 5 μg/mL Gentamicin) supplemented with 1 mM nonessential amino acids and 1 mM sodium pyruvate and incubated for 72 h at 37 °C in the presence of 20 ng/mL PMA. In several experiments, the human lung adenocarcinoma epithelial A549 cell line (ATCC) was used as a model of human type II alveolar epithelial cells and cultured as described in ref. 10. Primary type 1 and type 2 macrophages were also used as representative primary phagocytes with distinct functional activity (50). To get M1 or M2 macrophages, peripheral blood mononuclear cells were isolated from human buffy coat preparations and monocytes were separated, as previously described (51). Monocytes were then suspended in complete medium and incubated for a further 5 d in 24-well plates at the concentration of 10^6 cells/mL in the absence or in the presence of 100 ng/mL GM-CSF or 20 ng/mL M-CSF (both from R&D Systems) to get MDM, M1 and M2, respectively. The M1 and M2 phenotype was then confirmed by ELISA by quantifying TNF-α, IL-6, and IL-10 (all from Thermo Scientific) release in the supernatant and by flow cytometry after staining with anti-CD14, anti-CD16, and anti-CD163 monoclonal antibodies (Fig. S9 *A* and *B*) (50). dTHP-1 cells, A549 cells, M1, and M2 were then washed and reconstituted in complete medium, before use in experiments. In all experiments, cells were exposed to one liposome per cell.

Infection and Evaluation of Intracellular Mycobacterial Growth. Differentiated THP-1 (5×10^5/well) and M1 and M2 (10^6/well) were exposed for 3 h to MTB H37Rv at the multiplicity of infection (MOI) of 1 in 24-well plates. After removal of extracellular bacilli, cells were stimulated with phosphatidylserine outside/phosphatidic acid inside (ABL/PA), phosphatidylserine outside/phosphatidylcholine inside (ABL/PC), phosphatidylcholine outside/ phosphatidic acid inside (PC/PA), or phosphatidylcholine outside/phosphatidylcholine inside (PC/PC) and cfu assays were performed at days 3 and 5 postinfection, as previously described (9). To ascertain whether phagolysosome maturation was responsible for intracellular mycobacterial killing, 10 μM chloroquine or 20 mM NH_4Cl was added to MTB-infected cells together with ABL/PA, as described in ref. 10. Finally, the role of ROS in intracellular mycobacterial killing was analyzed by adding 100 units/mL PEG-Catalase.

Quantification of Cytokines by Real-Time PCR and ELISA. RNA extraction and real-time PCR were performed as previously described (52). Briefly, total RNA was extracted from 2×10^6 cells, using RNeasy kits (Qiagen) as described by the manufacturer, and quantified by optical density. One hundred nanograms of total RNA was reverse transcribed using the high-capacity cDNA Archive Kit (Applied Biosystems) and random hexamer primers in an ABI Prism 7000 Sequence Detector System (Applied Biosystems), using the following thermal profile: 25 °C for 10 min, 42 °C for 1 h, and 95 °C for 5 min. PCR reactions were performed in triplicate using TaqMan chemistry with primer and probe sets from the Assay-on-Demand list (Applied Biosystems). Each gene profile was compared with the standard curve of the reference and calculation of the slope of log[ng RNA] vs. ΔCt was always <0.1. Fold induction was then calculated by $\Delta\Delta Ct$ method (53), using the 18S mRNA level to normalize values and the mRNA level of basal condition (unstimulated dTHP-1) as a calibrator. Values of fold induction were the means ± SD of three independent cellular experiments.

The levels of IL-1β, TNF-α, and TGF-β in the supernatant of dTHP-1 cells infected or not with MTB at the MOI of 1 and stimulated or not with ABL/PA were assessed by commercially available kits [human TNF-α ELISA kit and human IL-1β ELISA kit (Thermo Scientific) and DRG TGF-β1 ELISA (DRG International)] and used according to the manufacturer's instructions.

Fluorimetric Analysis. The efficiency of liposome internalization by different cell types (A549, dTHP-1, MDM, M1, and M2) was analyzed by comparing fluorescence emission of cells before and after 90 min exposure to ABL carrying NBD-PA. In several experiments, the possible contribution of serum opsonization in liposome internalization was investigated by exposing cells to ABL/PA-NBD or PC/PA-NBD liposomes in the presence of complete medium supplemented with 10% FBS or 10% AB human serum. Percentage of the liposome internalized was calculated according to the following formula: [fluorescence arbitrary units (FAU) of cells exposed to liposome carrying

NBD-PA – FAU of control cells)/(FAU of liposome carrying NBD-PA – FAU of control cells] × 100.

Finally, intracellular Ca^{2+} was measured after labeling cells with the 3-μM fluorescent intracellular Ca^{2+} indicator Fluo-3/AM (Molecular Probes), as described in ref. 10, followed by incubation at 37 °C with the different liposome preparations used at the ratio of one liposome per cell. The concentration of Ca^{2+} was determined from fluorescence ratios, as previously described (54).

Fluorescence emission was monitored by the use of a Perkin-Elmer LS50B luminescence spectrometer.

Confocal Microscopy Analysis. The degree of maturation of MTB-containing endosomes was assessed after 18 h stimulation of dTHP-1 cells with ABL/PA or PC/PC, in presence or absence of 3 mM EGTA or 10 mM chloroquine, by analyzing the colocalization of bacilli with lysosomes after staining the mycobacteria with auramine and the lysosomes with (*i*) the acidophilic dye Lysotracker Red (Molecular Probes) (49), (*ii*) Alexa Fluor 647 anti-LAMP-3 monoclonal antibody (IgG1, clone MX-49.129.5; Santa Cruz Biotechnology), (*iii*) Alexa Fluor 647 anti-LAMP-1 monoclonal antibody (IgG2b, clone 25; Transduction Laboratories, Becton Dickinson), or (*iv*) anti-LC3 purified rabbit polyclonal antibody (clone name RB7481; Abgent). Briefly, cells were washed with PBS, fixed by 10 min incubation with 4% paraformaldehyde at 4 °C, and permeabilized with 0.2% Triton X-100 followed by further three washings with PBS. The localization of MTB was determined by incubating the infected monolayer with Auramine (Becton Dickinson) for 20 min at room temperature, followed by 3 min incubation in 0.5% acid alcohol and repeated washing with PBS. Detection of the lysosomal protein markers LAMP-1 and LAMP-3 was accomplished by 1 h incubation with specific monoclonal antibodies, and LC3 was analyzed by 1 h incubation with a polyclonal antibody stained with secondary antibody Alexa Fluor 488-conjugated anti-rabbit IgG for 1 h (Molecular Probes). In several experiments, the cells were incubated with 10 μg/mL DQ red BSA (Molecular Probes) for 2 h before infection and for 35 min after infection, at 37 °C. Detection of the acidophilic dye Lysotracker Red was analyzed on dTHP-1 cells infected for 3 h with MTB expressing green fluorescent protein (GFP-MTB) (55) and followed by 2 h incubation with the acidophilic dye. Then, cells were fixed and processed for confocal microscopy as indicated above.

Finally, in several experiments the internalization of liposomes was analyzed by confocal laser scanning microscopy, using a Leica TCS-SP5 operating system. The percentage of liposome-positive dTHP-1 cells was assessed by counting cells incorporating at least one liposome carrying NBD-PA over the total cells.

Efficacy of ABL/PA in BAL Cells. Three (age 40 ± 10 y, 3 males) of 13 patients enrolled for microbiological confirmation of pulmonary TB, before the initiation of antimycobacterial treatment, were finally diagnosed as active pulmonary TB with BAL culture positive for MTB. A fourth patient with infiltrated upper right lobe and one calcification on the left lower lobe at chest X-rays and BAL culture positive for ampicillin-resistant *K. pneumoniae* was also enrolled. Patients gave informed consent under a study protocol approved by the Ethics Committee of the National Institute of Infectious Diseases "Lazzaro Spallanzani," Rome, of the "Azienda Ospedaliera S. Camillo-Forlanini," Rome, and of Policlinico of "Tor Vergata," Rome. BAL was treated as previously described (11, 12). Briefly, BAL cells were suspended as 10^6 cells/mL in medium consisting of RPMI 1640 supplemented with 10% FBS, 2 mM L-Glu, 5 μg/mL Gentamycin, 5 μg/mL Ampicillin, and 2 μg/mL Fluconazole (all from Invitrogen) to allow selective growth of intracellular mycobacteria. Finally, 10^6 cells per well were incubated for 72 h in 24-well plates in the presence or absence of ABL/PA and analyzed at the time indicated by colony-forming unit assays, as previously described (11, 12).

Mice, Infection, and Treatments. BALB/c mice (Charles River Laboratories) were kept under specific pathogen-free conditions and used in accordance with institutional guidelines in compliance with national and international law and policies (56). Experiments were performed in specific pathogen-free facilities. Six mice per group (matched for sex and age between 8 and 10 wk) were infected (under light anesthesia) intranasally (i.n.) with 2.5×10^5 cfu of midlog-phase MTB H37Rv in 0.02 mL of saline. Starting from day 14 after infection and for a further 4 wk, mice received or not (*i*) 25 mg of INH (Sigma) per 100 mL of drinking water; (*ii*) intranasal inoculation of 10^5 ABL/PA, suspended in 50 μL of phosphate buffered saline, three times per week; or (*iii*) the combination of both treatments. At the end of the fourth and sixth week after infection, mice were killed, sera were collected, and tissue bacillary load of lungs, spleens, and livers was quantified by plating serial dilution of the lung, liver, and spleen homogenates into 7H10 agar, as described previously (56, 57). TNF-α, IL-1β, and IFN-γ were quantified in the sera (58) by ELISA kits (R&D Systems), used according to the manufacturer's instructions.

Statistical Analysis. Statistical analysis was carried out by the Graphpad Prism 3.0 software package. Comparison between groups was done using Student's *t* test. $P < 0.05$ was considered statistically significant.

ACKNOWLEDGMENTS. We thank the members of the laboratories for helpful discussions. We also thank the patients for the generosity given to participate in this study. This work was supported by (*i*) Italian Program of AIDS Research Grant N 40H45, (*ii*) Italian Ministry for University Progetti di Ricerca di Interesse Nazionale (PRIN) Grant 2008L57JXW_005, (*iii*) The Netherlands Organization of Scientific Research, (*iv*) 7th Framework Programme of European Commission "Discovery and Preclinical Development of New Vaccine Candidates for Tuberculosis (NEWTBVAC)" Grant 241745, and (*v*) Bill and Melinda Gates Foundation Grand Challenges in Global Health Grant GC6#74.

1. Steinberg BE, Grinstein S (2008) Pathogen destruction versus intracellular survival: The role of lipids as phagosomal fate determinants. *J Clin Invest* 118:2002–2011.
2. Kusner DJ, Adams J (2000) ATP-induced killing of virulent *Mycobacterium tuberculosis* within human macrophages requires phospholipase D. *J Immunol* 164:379–388.
3. Coutinho-Silva R, et al. (2003) Inhibition of chlamydial infectious activity due to P2X7R-dependent phospholipase D activation. *Immunity* 19:403–412.
4. Auricchio G, et al. (2003) Role of macrophage phospholipase D in natural and CpG-induced antimycobacterial activity. *Cell Microbiol* 5:913–920.
5. Yeung T, Grinstein S (2007) Lipid signaling and the modulation of surface charge during phagocytosis. *Immunol Rev* 219:17–36.
6. Malik ZA, et al. (2003) Cutting edge: *Mycobacterium tuberculosis* blocks Ca^{2+} signaling and phagosome maturation in human macrophages via specific inhibition of sphingosine kinase. *J Immunol* 170:2811–2815.
7. Fratti RA, Chua J, Vergne I, Deretic V (2003) *Mycobacterium tuberculosis* glycosylated phosphatidylinositol causes phagosome maturation arrest. *Proc Natl Acad Sci USA* 100:5437–5442.
8. Anes E, et al. (2003) Selected lipids activate phagosome actin assembly and maturation resulting in killing of pathogenic mycobacteria. *Nat Cell Biol* 5:793–802.
9. Garg SK, et al. (2004) Sphingosine 1-phosphate induces antimicrobial activity both in vitro and in vivo. *J Infect Dis* 189:2129–2138.
10. Greco E, et al. (2010) Natural lysophospholipids reduce *Mycobacterium tuberculosis*-induced cytotoxicity and induce anti-mycobacterial activity by a phagolysosome maturation-dependent mechanism in A549 type II alveolar epithelial cells. *Immunology* 129:125–132.
11. Garg SK, et al. (2006) Does sphingosine 1-phosphate play a protective role in the course of pulmonary tuberculosis? *Clin Immunol* 121:260–264.
12. Garg SK, et al. (2006) Lysophosphatidic acid enhances antimycobacterial activity both in vitro and ex vivo. *Clin Immunol* 121:23–28.
13. Delogu G, et al. (2011) Lysophosphatidic acid enhances antimycobacterial response during in vivo primary *Mycobacterium tuberculosis* infection. *Cell Immunol* 271:1–4.
14. Grimsley C, Ravichandran KS (2003) Cues for apoptotic cell engulfment: Eat-me, don't eat-me and come-get-me signals. *Trends Cell Biol* 13:648–656.
15. Schlegel RA, Williamson P (2001) Phosphatidylserine, a death knell. *Cell Death Differ* 8:551–563.
16. Krahling S, Callahan MK, Williamson P, Schlegel RA (1999) Exposure of phosphatidylserine is a general feature in the phagocytosis of apoptotic lymphocytes by macrophages. *Cell Death Differ* 6:183–189.
17. Birge RB, Ucker DS (2008) Innate apoptotic immunity: The calming touch of death. *Cell Death Differ* 15:1096–1102.
18. Erwig LP, Henson PM (2007) Immunological consequences of apoptotic cell phagocytosis. *Am J Pathol* 171:2–8.
19. Pautot S, Frisken BJ, Weitz DA (2003) Engineering asymmetric vesicles. *Proc Natl Acad Sci USA* 100:10718–10721.
20. Kooijman EE, Chupin V, de Kruijff B, Burger KN (2003) Modulation of membrane curvature by phosphatidic acid and lysophosphatidic acid. *Traffic* 4:162–174.
21. Tendian SW, Lentz BR (1990) Evaluation of membrane phase behavior as a tool to detect extrinsic protein-induced domain formation: Binding of prothrombin to phosphatidylserine/phosphatidylcholine vesicles. *Biochemistry* 29:6720–6729.
22. Greco E, et al. (2006) CpG oligodeoxynucleotides induce Ca^{2+}-dependent Phospholipase D leading to phagolysosome maturation and mycobacteriocidal activity in monocytes. *Biochem Biophys Res Commun* 347:963–969.
23. Malik ZA, Denning GM, Kusner DJ (2000) Inhibition of Ca(2+) signaling by *Mycobacterium tuberculosis* is associated with reduced phagosome-lysosome fusion and increased survival within human macrophages. *J Exp Med* 191:287–302.
24. Flynn JL (2004) Immunology of tuberculosis and implications in vaccine development. *Tuberculosis (Edinb)* 84:93–101.
25. Kaufmann SH (2001) How can immunology contribute to the control of tuberculosis? *Nat Rev Immunol* 1:20–30.
26. Ottenhoff TH (2009) Overcoming the global crisis: "Yes, we can", but also for TB . . .? *Eur J Immunol* 39:2014–2020.
27. Babior BM (2004) NADPH oxidase. *Curr Opin Immunol* 16:42–47.

28. Rybicka JM, Balce DR, Khan MF, Krohn RM, Yates RM (2010) NADPH oxidase activity controls phagosomal proteolysis in macrophages through modulation of the lumenal redox environment of phagosomes. *Proc Natl Acad Sci USA* 107:10496–10501.
29. Verreck FA, et al. (2004) Human IL-23-producing type 1 macrophages promote but IL-10-producing type 2 macrophages subvert immunity to (myco)bacteria. *Proc Natl Acad Sci USA* 101:4560–4565.
30. Mantovani A, Sica A, Locati M (2005) Macrophage polarization comes of age. *Immunity* 23:344–346.
31. Redente EF, et al. (2010) Differential polarization of alveolar macrophages and bone marrow-derived monocytes following chemically and pathogen-induced chronic lung inflammation. *J Leukoc Biol* 88:159–168.
32. Felnerova D, Viret JF, Glück R, Moser C (2004) Liposomes and virosomes as delivery systems for antigens, nucleic acids and drugs. *Curr Opin Biotechnol* 15:518–529.
33. Gardell SE, Dubin AE, Chun J (2006) Emerging medicinal roles for lysophospholipid signaling. *Trends Mol Med* 12:65–75.
34. Flynn JL, Chan J, Lin PL (2011) Macrophages and control of granulomatous inflammation in tuberculosis. *Mucosal Immunol* 4:271–278.
35. Davis JM, Ramakrishnan L (2009) The role of the granuloma in expansion and dissemination of early tuberculous infection. *Cell* 136:37–49.
36. Maderna P, Godson C (2003) Phagocytosis of apoptotic cells and the resolution of inflammation. *Biochim Biophys Acta* 1639:141–151.
37. Huynh ML, Fadok VA, Henson PM (2002) Phosphatidylserine-dependent ingestion of apoptotic cells promotes TGF-beta1 secretion and the resolution of inflammation. *J Clin Invest* 109:41–50.
38. Marriott HM, et al. (2006) Decreased alveolar macrophage apoptosis is associated with increased pulmonary inflammation in a murine model of pneumococcal pneumonia. *J Immunol* 177:6480–6488.
39. Teder P, et al. (2002) Resolution of lung inflammation by CD44. *Science* 296:155–158.
40. Deretic V, et al. (2006) *Mycobacterium tuberculosis* inhibition of phagolysosome biogenesis and autophagy as a host defence mechanism. *Cell Microbiol* 8:719–727.
41. Melendez AJ, Allen JM (2002) Phospholipase D and immune receptor signalling. *Semin Immunol* 14:49–55.
42. Ramachandra L, Simmons D, Harding CV (2009) MHC molecules and microbial antigen processing in phagosomes. *Curr Opin Immunol* 21:98–104.
43. Sly LM, Lopez M, Nauseef WM, Reiner NE (2001) 1alpha,25-Dihydroxyvitamin D3-induced monocyte antimycobacterial activity is regulated by phosphatidylinositol 3-kinase and mediated by the NADPH-dependent phagocyte oxidase. *J Biol Chem* 276:35482–35493.
44. Yang CS, et al. (2009) NADPH oxidase 2 interaction with TLR2 is required for efficient innate immune responses to mycobacteria via cathelicidin expression. *J Immunol* 182: 3696–3705.
45. Huang J, et al. (2009) Activation of antibacterial autophagy by NADPH oxidases. *Proc Natl Acad Sci USA* 106:6226–6231.
46. Shahnazari S, et al. (2010) A diacylglycerol-dependent signaling pathway contributes to regulation of antibacterial autophagy. *Cell Host Microbe* 8:137–146.
47. Mosser DM (2003) The many faces of macrophage activation. *J Leukoc Biol* 73: 209–212.
48. Serezani CH, Aronoff DM, Jancar S, Mancuso P, Peters-Golden M (2005) Leukotrienes enhance the bactericidal activity of alveolar macrophages against *Klebsiella pneumoniae* through the activation of NADPH oxidase. *Blood* 106:1067–1075.
49. Finlay BB, Hancock RE (2004) Can innate immunity be enhanced to treat microbial infections? *Nat Rev Microbiol* 2:497–504.
50. Verreck FA, de Boer T, Langenberg DML, van der Zanden L, Ottenhoff THM (2006) Phenotypic and functional profiling of human proinflammatory type-1 and anti-inflammatory type-2 macrophages in response to microbial antigens and IFN-gamma- and CD40L-mediated costimulation. *J Leukoc Biol* 79:285–293.
51. Ciaramella A, et al. (2004) Induction of apoptosis and release of interleukin-1 beta by cell wall-associated 19-kDa lipoprotein during the course of mycobacterial infection. *J Infect Dis* 190:1167–1176.
52. Ciccaglione AR, et al. (2008) Microarray analysis identifies a common set of cellular genes modulated by different HCV replicon clones. *BMC Genomics* 9:309–320.
53. Livak KJ, Schmittgen TD (2001) Analysis of relative gene expression data using real-time quantitative PCR and the 2(-Delta Delta C(T)) method. *Methods* 25:402–408.
54. Grynkiewicz G, Poenie M, Tsien RY (1985) A new generation of Ca^{2+} indicators with greatly improved fluorescence properties. *J Biol Chem* 260:3440–3450.
55. Delogu G, et al. (2004) Rv1818c-encoded PE_PGRS protein of *Mycobacterium tuberculosis* is surface exposed and influences bacterial cell structure. *Mol Microbiol* 52:725–733.
56. Di Liberto D, et al. (2008) Role of the chemokine decoy receptor D6 in balancing inflammation, immune activation, and antimicrobial resistance in *Mycobacterium tuberculosis* infection. *J Exp Med* 205:2075–2084.
57. Dieli F, et al. (2003) Characterization of lung $\gamma\,\delta$ T cells following intranasal infection with *Mycobacterium bovis* bacillus Calmette-Guérin. *J Immunol* 170:463–469.
58. Garlanda C, et al. (2007) Damping excessive inflammation and tissue damage in *Mycobacterium tuberculosis* infection by Toll IL-1 receptor 8/single Ig IL-1-related receptor, a negative regulator of IL-1/TLR signaling. *J Immunol* 179:3119–3125.